Intersystem Crossing Mediated by Photoinduced Intramolecular Charge Transfer: Julolidine−Anthracene Molecules with Perpendicular π Systems

Zachary E. X. Dance, Sarah M. Mickley, Thea M. Wilson, Annie Butler Ricks, Amy M. Scott, Mark A. Ratner,* and Michael R. Wasielewski*

Department of Chemistry, Argonne-Northwestern Solar Energy Research (ANSER) Center, and International Institute of Nanotechnology, Northwestern University, Evanston, Illinois, 60208-3113

Received: January 20, 2008; In Final Form: February 19, 2008

Time-resolved electron paramagnetic resonance studies show that the primary mechanism of triplet formation following photoexcitation of julolidine-anthracene molecules linked by a single bond and having perpendicular π systems is a spin−orbit, charge-transfer intersystem crossing mechanism (SOCT−ISC). This mechanism depends on the degree of charge transfer from julolidine to anthracene, the dihedral angle (θ_1) between their π systems, and the magnitude of the electronic coupling between julolidine and anthracene. We compare 4-(9-anthracenyl)-julolidine with the more sterically encumbered 4-(9-anthracenyl)-3,5-dimethyljulolidine and find that fixing $\theta_1 \cong 90°$ serves to enhance SOCT−ISC by increasing the change in orbital angular momentum accompanying charge transfer. Given that the requirements for the SOCT−ISC mechanism are quite general, we expect it to occur in a variety of electron donor−acceptor systems.

Introduction

In the past four decades, the photophysics of electron donor−acceptor (D-A) molecules covalently linked by a single bond have been studied extensively.[1] A large fraction of this work has been directed toward understanding the electronic structures and conformations of these molecules in their ground and lowest excited singlet charge-transfer (CT) states.[1−14] These molecules usually display CT absorption and emission bands and exhibit large excited-state dipole moments, which imply that the electronic coupling matrix element between the donor and the acceptor, V_{DA}, is reasonably large and that significant electron density is transferred from the donor to the acceptor in the excited state. One particular group of molecules that fulfills these criteria are 4-(9-anthryl)-*N*,*N*-dimethylaniline (ADMA) derivatives.[2−16] The nature of the ADMA excited CT state has been studied by Okada et al.[17] and Herbich et al. [3,18] and the relevant issues have been summarized by Grabowski et al. [1,19] Many of these studies have examined ADMA derivatives with substituents that sterically control rotations about the nitrogen−phenyl or phenyl−anthracene single bonds to simplify the photophysics exhibited by ADMA itself. For example, in julolidine−anthracene (J−An), Figure 1, the structure of julolidine severely restricts rotation about the nitrogen−phenyl single bond, which maximizes the overlap of the nitrogen lone pair with the π system of the phenyl ring.[2] This leaves the julolidine−anthracene torsional angle, θ_1, in J−An as a key parameter that determines its excited-state properties.[11,12,20−22]

Despite the attention ADMA systems have received, there have been relatively few studies on the mechanism of radiationless decay of their CT states.[2,23] As is usually the case, this decay can occur by internal conversion to the ground state or intersystem crossing (ISC) to the triplet manifold, Figure 2. In the present work, we explore the ISC mechanism associated with the formation of the triplet state localized on anthracene following photoexcitation into the CT absorption bands of

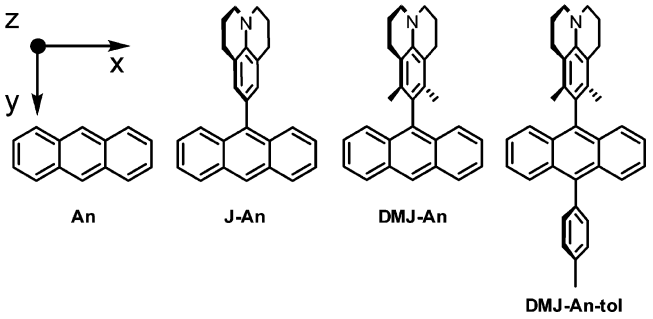

Figure 1. Principal axis system and molecular structures of anthracene and its julolidine-substituted derivatives.

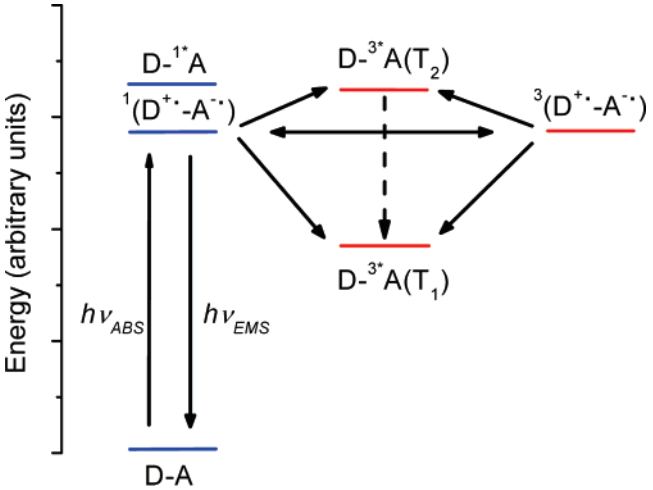

Figure 2. Energy level ordering for J-An, DMJ-An, and DMJ-An-tol, where D = J or DMJ, and A = An.

J−An, DMJ−An, and DMJ−An−tol, Figure 1. DMJ−An is modeled after J−An, but uses additional methyl groups on julolidine to enforce a geometry in which the π system of DMJ is perpendicular to that of the anthracene, i.e., $\theta_1 \approx 90°$. DMJ−

* Corresponding author. E-mail: m-wasielewski@northwestern.edu.

10.1021/jp800561g CCC: $40.75
Published on Web 04/03/2008

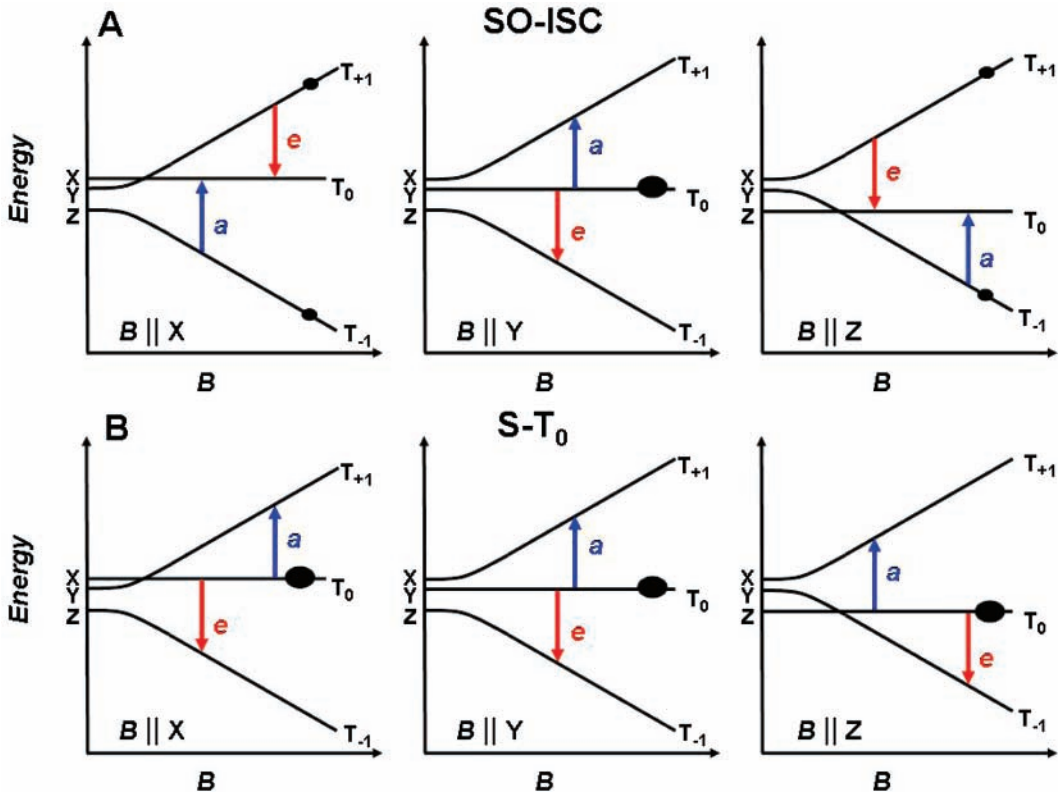

Figure 3. Energy levels of D-^{3*}A formed by (A) SO−ISC with selective population of T_Y ($D > 0$, $E < 0$) and (B) S−T_0 mixing within a radical pair precursor. The arrows indicate the direction of the transition and are labeled a = enhanced absorption, e = emission. The solid ovals depict relative populations.

An−tol was also studied as a control molecule because 9-phenyl and 9,10-diphenyl substitution of anthracene have been shown to dramatically reduce its ISC yield.[24−33]

A detailed analysis of the ISC mechanism in J−An, DMJ−An, and DMJ−An−tol requires consideration of the nature of their CT states, which can be represented as a mixture of the locally excited (LE) states of the anthracene acceptor and the radical ion pair (RP) states shown in Figure 2 and expressed in eq 1[1,13,34−39] where $\Sigma c_i^2 = 1$. The energies of the ground state

$$\Psi_{CT} = c_{1^*_A}\phi_{1^*_A} + c_{3^*_{A(T1)}}\phi_{3^*_{A(T1)}} + c_{3^*_{A(T2)}}\phi_{3^*_{A(T2)}} + c_{1_{(D^{+\bullet}A^{-\bullet})}}\phi_{1_{(D^{+\bullet}A^{-\bullet})}} + c_{3_{(D^{+\bullet}A^{-\bullet})}}\phi_{3_{(D^{+\bullet}A^{-\bullet})}} \quad (1)$$

and the LE states of the julolidine donor are well separated from those of the RP states, $^1(D^{+\bullet}-A^{-\bullet})$ and $^3(D^{+\bullet}-A^{-\bullet})$, so that these LE states should not contribute significantly to Ψ_{CT}. In contrast, the contribution of the lowest excited LE singlet state of the anthracene acceptor, ^{1*}A, as well as its two lowest LE triplet states, $^{3*}A(T_1)$ and $^{3*}A(T_2)$, to Ψ_{CT} may be more significant because they are energetically much closer to $^1(D^{+\bullet}-A^{-\bullet})$ and $^3(D^{+\bullet}-A^{-\bullet})$. Both of these RP states may also be important to the overall mechanism leading to the formation of D−^{3*}A.

When $^1(D^{+\bullet}-A^{-\bullet})$ dominates the overall electronic description of the Franck−Condon CT state produced upon photoexcitation, Figure 2, two ISC mechanisms distinct from ordinary spin−orbit induced ISC (SO−ISC) typical of LE singlet states in aromatic molecules may yield a triplet state localized on D or A. One mechanism, radical pair-intersystem crossing (RP-ISC), involves mixing between the $^1(D^{+\bullet}-A^{-\bullet})$ and $^3(D^{+\bullet}-A^{-\bullet})$ states induced by electron−nuclear hyperfine coupling within the two radicals. The theory and mechanistic details of RP-ISC have been researched extensively[40−44] and have been applied to many donor−acceptor systems.[45−53] This mechanism is generally important when the singlet−triplet energy splitting, $2J$, between $^1(D^{+\bullet}-A^{-\bullet})$ and $^3(D^{+\bullet}-A^{-\bullet})$ is smaller than the sum of the hyperfine couplings in $D^{+\bullet}$ and $A^{-\bullet}$. RP-ISC is usually followed by spin-selective charge recombination to produce a significant yield of the lowest neutral molecular triplet state, in this case D−^{3*}A. Alternatively, intersystem crossing from $^1(D^{+\bullet}-A^{-\bullet})$ may take place via a spin−orbit coupling mechanism to produce the neutral triplet state directly, Figure 2, provided that the symmetries of the orbitals involved in the charge transfer are such that the spin flip is coupled to a significant change in orbital angular momentum.[35,54−57] Whether either of these ISC mechanisms involves formation of the T_2 state of the acceptor, followed by internal conversion to its T_1 state, and/or direct formation of the T_1 state, depends on the energetic proximity of T_2 to $^1(D^{+\bullet}-A^{-\bullet})$ and $^3(D^{+\bullet}-A^{-\bullet})$ and will be discussed below.

Time-resolved electron paramagnetic resonance (TREPR) techniques, which are particularly well-suited for investigating the behavior of CT mechanisms involving paramagnetic states,[44,58−69] were used to examine the triplet states of An, J−An, DMJ−An, and DMJ−An−tol. Application of a magnetic field results in Zeeman splitting of the triplet sublevels, which at low fields are best described by the zero-field eigenstates, T_X, T_Y, and T_Z that are quantized in the molecular framework, and at high fields by the T_{+1}, T_0, and T_{-1} eigenstates that are quantized along the applied magnetic field, Figure 3. The main features of the EPR spectrum of D−^{3*}A arise from zero-field splitting (ZFS), which is a result of the magnetic dipole−dipole interaction between the two unpaired electrons in the triplet state. The Hamiltonian that describes this interaction is[70−73]

$$\mathscr{H}_{dipolar} = D(\mathbf{S}_z^2 - \mathbf{S}^2/3) + E(\mathbf{S}_x^2 - \mathbf{S}_y^2) \quad (2)$$

where D and E are the zero-field-splitting parameters and $\mathbf{S}_{x,y,z}$ are the components of the total spin angular momentum operator ($\mathbf{S}$) for the triplet state. The effect of this term is to lift the degeneracy of the triplet manifold in the absence of an external magnetic field as a function of the symmetry of the molecule. The polarization of the EPR transitions exhibited by D−^{3*}A formed by the SO−ISC mechanism can be differentiated from the RP-ISC mechanism by the electron spin polarization (ESP) pattern of the six EPR transitions, i.e., the two transitions at each canonical (x, y, z) orientation.[74] In SO−ISC, the three zero-field levels T_X, T_Y, and T_Z of D−^{3*}A are selectively populated and this selectivity is carried over to the high-field energy levels. For example, assuming selective population of the T_Y zero-field level and $D > 0$, Figure 3A shows that the six EPR transitions from low to high field yield an (*e*, *a*, *e*, *a*, *e*, *a*) polarization pattern, where *a* = enhanced absorption and *e* = emission of microwave radiation. In contrast, RP-ISC acts directly on the high-field triplet sublevels of the RP via S−T_0 mixing, Figure 3B. Spin polarization is preserved upon charge recombination, and the resulting (*a*, *e*, *e*, *a*, *a*, *e*) polarization pattern exhibited by D−^{3*}A is the unique signature of the RP-ISC mechanism.

Experimental Section

Zone-refined An (Aldrich) was used without further purification. The syntheses and characterization of J−An,[2] DMJ−An, and DMJ−An−tol are given in the Supporting Information. J−An, DMJ−An, and DMJ−An−tol were purified by preparative TLC prior to use. A 10 mm path length quartz cuvette was used for both the absorption and fluorescence measurements, and the optical density at $\lambda_{max}$for the fluorescence measurements was maintained at $<0.1 \pm 0.05$ to avoid reabsorption artifacts. Samples for steady state and time-resolved fluorescence measurements as well as nanosecond transient absorption measurements were subjected to several freeze−pump−thaw degassing cycles on a vacuum line (1×10^{-4} Torr). Steady state absorption and emission spectra were performed on a Shimadzu 1601 UV/vis spectrophotometer and PTI single photon counting spectrofluorimeter, respectively. Emission quantum yields were determined relative to that of quinine sulfate, $\phi_F = 0.546$ in 0.5 M H_2SO_4.[75]

Fluorescence lifetime measurements were made using a Hamamatsu C4780 picosecond fluorescence lifetime measurement system, consisting of a C4334 Streakscope and a C4792−01 synchronous delay generator. The excitation light source was supplied by a home-built cavity-dumped Ti:sapphire laser[76] with a NEOS N13389 3-mm fused-silica acoustooptic modulator (AOM). The AOM was driven by an NEOS Technologies N64389-SYN 10 W driver to deliver 30 nJ, sub-50 fs pulses at an 820 kHz repetition rate. The laser pulses were frequency doubled to 400 nm by focusing the 800 nm fundamental into a 0.3 mm type I BBO crystal. The energy of the resulting blue pulses was attenuated to approximately 0.5 nJ/pulse for all fluorescence lifetime experiments. The total instrument response function (IRF) of the streak camera system was 20 ps. All fluorescence data were acquired in single-photon-counting mode using the Hamamatsu HPD-TA software. The data were fit using the Hamamatsu fitting module and deconvoluted using the laser pulse profile.

Nanosecond transient absorption measurements were made using a Continuum Panther OPO pumped by the frequency-tripled output of a Continuum 8000 Nd:YAG laser. The probe light in the nanosecond experiment was generated using a xenon flashlamp (EG&G Electrooptics FX-200) and detected using a photomultiplier tube with high voltage applied to only four dynodes (Hamamatsu R928). The total IRF is 7 ns and is determined primarily by the laser pulse duration. Triplet quantum yields, ϕ_{ISC}, were obtained from the amplitude of the transient absorption change at 430 nm and the extinction coefficient of ^{3*}An.[77]

Samples for TREPR (∼1 mM in toluene) were loaded in 4 mm OD × 2 mm ID quartz tubes and subjected to several freeze−pump−thaw degassing cycles on a vacuum line (1×10^{-4} Torr). The tubes were then sealed with a hydrogen torch. All samples were prepared in freshly distilled ACS grade toluene.

TREPR field-swept electron spin echo (ESE) measurements of the triplet EPR spectra were made using a Bruker Elexsys E580 X-Band EPR spectrometer outfitted with a variable Q dielectric resonator (ER-4118X-MD4-W1). High-power microwave pulses were generated by a 1 kW TWT amplifier (Applied Systems Engineering 117X). The resonator was fully overcoupled to achieve $Q < 200$ and a dead time of ∼68 ns. The temperature was controlled by an Oxford Instruments CF935 continuous flow cryostat using liquid nitrogen or helium. Samples were photoexcited at 416 nm (355 nm for anthracene) using the output from a frequency tripled, H_2-Raman shifted Nd:YAG laser (1−2 mJ/pulse, 7 ns, 10 Hz, QuantaRay DCR-2). The polarization of the laser was set to 54.7° relative to the direction of the static magnetic field to avoid magnetophotoselection effects on the spectra.

In the basic Hahn-echo technique,[58] the FID signal generated with the first 8 ns $\pi/2$ pulse is refocused by a second 16-ns π pulse. The time between the two microwave pulses was 68 ns, so that the spin echo appears 68 ns following the second microwave pulse. The microwave pulse sequence begins after the triplet state is created by the laser pulse. Following photoexcitation, the integral of the echo intensity at a given delay time at each magnetic field value gives the spectrum of the spin-polarized triplets. Microwave signals in emission (*e*) and/or enhanced absorption (*a*) were detected in both the real and the imaginary channels (quadrature detection). Four-step phase cycling was performed in order to suppress artifacts due to imbalances in the quadrature detection. Sweeping the magnetic field gave 2D complex spectra versus time and magnetic field. The spectra were subsequently phased into a Lorentzian part and a dispersive part, and the former, also known as the imaginary magnetic susceptibility χ'', is presented. Simulation of the powder-pattern spectra of the spin-polarized triplet states was performed using a home-written MATLAB program[78] following published procedures.[72]

Results and Discussion

Photophysical Properties of Singlet CT States. The ground-state absorption (A) and fluorescence (F) spectra of J−An, DMJ−An, and DMJ−An−tol, plotted in their respective transition dipole moment representations,[79] i.e., $A(\bar{\nu})/\bar{\nu}$ and $F(\bar{\nu})/\bar{\nu}^3$, are given in Figure 4. The CT absorption band of J−An appears as a distinct shoulder on the vibronic progression of the anthracene LE state,[3] whereas those of DMJ−An and DMJ−An−tol appear as significant broadening on the red edge of their spectra. Each absorption spectrum can be decomposed into a sum of Gaussians both to account for the anthracene Franck−Condon progression and to fit the broad CT absorption of each molecule. The absorption maxima of the CT bands obtained in this manner are given in Table 1. The fluorescence spectra for J−An, DMJ−An, and DMJ−An−tol are all strongly red-shifted relative to the emission from the An LE state and are

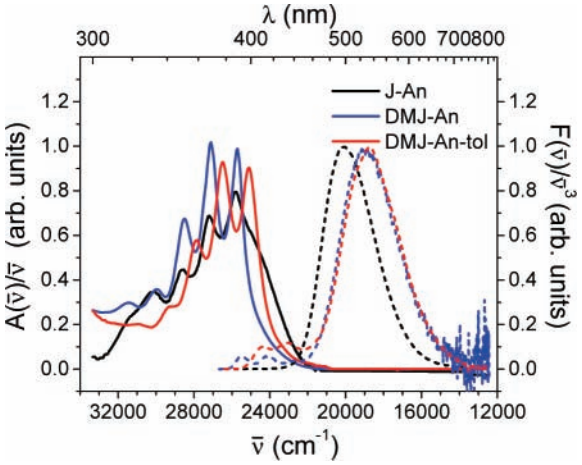

Figure 4. Ground-state absorption (solid lines) and fluorescence spectra (dashed lines) of the indicated molecules in toluene. The fluorescence spectra are normalized at their maxima.

characteristic of CT emission as observed earlier for J−An.[3] The energies of the LE and CT states are obtained by averaging the energies of their absorption and emission bands, Table 1. Given that the energy of the LE absorption maximum of J−An is nearly identical to that of DMJ-An, we assume that the energies of their LE states are comparable, even though LE emission from J−An was not observed.

The excited-state dipole moments (μ_e) of DMJ−An and DMJ−An−tol were determined by the fluorescence solvatochromic shift method,[80,81] using eq 3

$$\bar{\nu}_{max} = \bar{\nu}_0 - \frac{2\mu_e^2}{hca_0^3}\left[\frac{(\epsilon - 1)}{(2\epsilon + 1)} - \frac{(n^2 - 1)}{2(2n^2 + 1)}\right] \qquad (3)$$

where h is Planck's constant, c is the speed of light, $\bar{\nu}_0$ is the gas-phase emission maximum, and $\bar{\nu}_{max}$ is the energy of the CT emission band measured in several solvents with dielectric constant ϵ and index of refraction n. The radius of the Onsager spherical cavity, a_0^3, was determined to be 6.5 Å using the PM3[82] optimized DMJ−An structure, which is in agreement with that previously estimated for J−An.[2] Using this value and the slope of the plot of $hc\bar{\nu}_{max}$ vs $[(\epsilon - 1)/(2\epsilon + 1) - 0.5(n^2 - 1)/(2n^2 + 1)]$, Figures S1 and S2 of the Supporting Information, $\mu_e = 26 \pm 1$ D for both DMJ−An and DMJ−An−tol. The same value of μ_e was obtained for J−An using the fluorescence data reported earlier[3] and $a_0 = 6.5$ Å. We estimate the degree of charge separation in the ^{1}CT state as 26 D/4.8 D esu^{-1} Å^{-1} = 5.4 esu Å. Using the centers of the spin density distributions in DMJ$^{+\bullet}$ and An$^{-\bullet}$, the distance that a full charge is transferred to yield DMJ$^{+\bullet}$−An$^{-\bullet}$ is 5.6 Å. Thus, the estimated percentage of charge separation in ^{1}CT is (5.4 esu Å/5.6 esu Å) × 100 = 96%. These data indicate that charge separation within the ^{1}CT states of J−An, DMJ−An, and DMJ−An−tol is essentially quantitative, so that their ^{1}CT states can be described by ^{1}(D$^{+\bullet}$−A$^{-\bullet}$).

The data in Table 1 show that the radiative rate constants, k_R, for DMJ−An and DMJ−An−tol are about 7−9 times smaller than that of J−An, whereas their corresponding intersystem crossing rate constants, k_{ISC}, are about 6−20 times larger. The most likely source of these rate differences are molecular properties that depend on the dihedral angle θ_1 between the π systems of the julolidine donors and that of An about the single bond joining them. Density functional theory (DFT) calculations[83] using the B3LYP[84,85] functional and the 6-31G* basis set have been used to determine the ground state values of θ_1 for J−An, DMJ−An, and DMJ−An−tol, Table 2. The value of θ_2, the tolyl−anthracene torsional angle in DMJ−An−tol, and the phenyl−anthracene angle in 9-phenylanthracene (9-PhAn), were obtained using the same methodology, Table 2. These calculations show that the π systems of the julolidine donor and the anthracene acceptor are nearly perpendicular ($\theta_1 \cong 90°$) for DMJ−An and DMJ−An−tol in both their singlet ground state and their lowest triplet state, whereas the corresponding angles for J−An are significantly smaller. Due to issues involving the accuracy of excited-state calculations, comparable calculations of the CT states were not attempted. However, it is likely that the conformational restrictions provided by the methyl groups in DMJ−An and DMJ−An−tol also result in larger dihedral angles between the π systems of DMJ and An in their CT states relative to that of J−An.

Changing θ_1 may impact the energies of both the LE and CT states, the symmetry-dependent selection rules for transitions between these states, and the electronic coupling matrix element between the donor and the acceptor, V_{DA}. The data in Table 1 show that the energies of the CT states for all three molecules are comparable, whereas the energy of the LE state of DMJ−An−tol is 0.11 eV lower than that of DMJ-An due to the additional conjugative interaction of the tolyl group. Thus, the energy differences between the LE and CT states for J−An, DMJ−An, and DMJ−An−tol are all about 0.3 eV, so that the observed differences in k_{ISC} more strongly reflect the effects of changing θ_1 on V_{DA} and orbital symmetry-based ISC selection rules. These issues will be discussed in the context of the TREPR data.

Triplet State TREPR Spectrum of Anthracene. Following direct photoexcitation into its LE absorption band, the observed TREPR spectrum of An in toluene at 85 K exhibits a broad triplet spectrum with a width of ∼150 mT, having an (*e*, *e*, *e*, *a*, *a*, *a*) ESP phase pattern, which results from a SO−ISC mechanism, Figure 5. The photophysical behavior of anthracene and its derivatives following photoexcitation has been studied extensively.[31,63,86−92] Experimental and theoretical[92] studies have shown the energetic order of anthracene's triplet sublevels to be $T_X > T_Y > T_Z$, such that the ZFS parameters $D > 0$ and $E < 0$, where the principal axis system is shown in Figure 1. Symmetry arguments suggest that T_X should be preferentially populated, however experimental evidence has shown that T_Y is also populated to a similar extent giving the (*e*, *e*, *e*, *a*, *a*, *a*) ESP phase pattern, Table 3.[63,64,91,92] Computer simulations of the triplet spectra for ^{3*}An confirm that the (*e*, *e*, *e*, *a*, *a*, *a*) ESP phase pattern is the result of the SO−ISC coupling mechanism with preferential population of both the T_Y and T_X sublevels for $D > 0$, $E < 0$.[93,94]

Triplet State TREPR Spectra of DMJ−An and DMJ−An−tol. In contrast to anthracene, the triplet spectra of DMJ−^{3*}An and DMJ−^{3*}An-tol both exhibit an (*e*, *a*, *e*, *a*, *e*, *a*) ESP phase pattern, Figure 5, whereas no triplet spectrum is observed for J−An following photoexcitation. The $|D|$ and $|E|$ values for DMJ−^{3*}An and DMJ−^{3*}An−tol are only slightly smaller than those of An indicating that the triplet excitation is localized on An. The ZFS parameters and the relative population rates of the triplet sublevels were determined by computer simulation of the triplet line shape and are presented in Table 3. It has been suggested for similar D−A systems that ISC resulting in the population of D−^{3*}A occurs via the triplet CT state.[2,11] This mechanism requires a high degree of charge separation, so that the initially formed CT state must be well described by ^{1}(D$^{+\bullet}$−A$^{-\bullet}$). As noted above, an analysis of the CT emission spectra of DMJ−An and DMJ−An−tol show that this criterion is

TABLE 1: Photophysical Data in Toluene

molecule	λ_{abs-LE} (nm)	λ_{ems-LE} (nm)	E_{LE} (eV)	λ_{abs-CT} (nm)	λ_{ems-CT} (nm)	E_{CT} (eV)	ϕ_{ems-CT}	τ_{ems-CT} (ns)	k_R[a] ($\times 10^7$ s^{-1})	ϕ_{ISC}	k_{ISC}[b] ($\times 10^7$ s^{-1})
J−An	388		3.18[c]	386	498	2.85	0.62	10.0 ± 0.1	6.2	<0.02	<0.05
DMJ−An	389	392	3.18	375	528	2.83	0.31	45.2 ± 0.1	0.69	0.45	1.0
DMJ−An−tol	399	410	3.07	391	533	2.75	0.40	42.0 ± 0.1	0.95	0.13	0.29

[a] $k_R = \phi_{ems-CT}/\tau_{ems-CT}$. [b] $k_{ISC} = \phi_{ISC}/\tau_{ems-CT}$. [c] Estimated from absorption data alone.

TABLE 2: Calculated Dihedral Angles[a]

molecule	singlet θ_1	singlet θ_2	triplet θ_1	triplet θ_2
J−An	75.1		56.9	
DMJ−An	89.6		89.6	
DMJ−An−tol	90.0	81.5	89.2	65.8
9−PhAn		86.9		67.5

[a] θ_1 is the angle between julolidine and anthracene; θ_2 is the angle between anthracene and the phenyl group (when present).

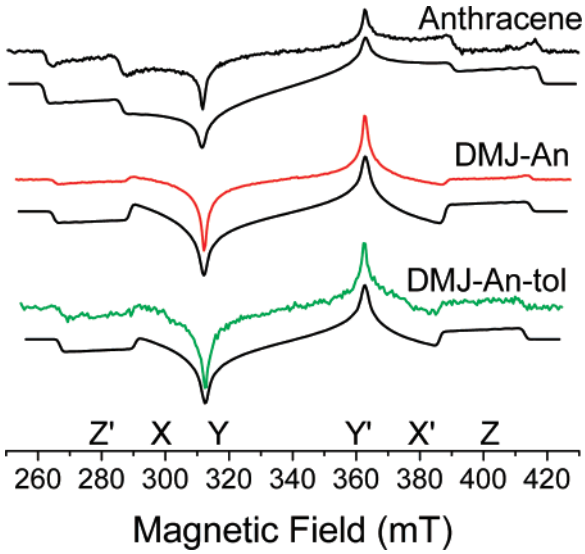

Figure 5. TREPR spectra of the indicated molecules in toluene at 85 K and 900 ns following a 416 nm (355 nm for An), 7 ns, 1.5 mJ laser pulse. The canonical orientations of each transition are indicated. Smooth curves below the experimental spectra are computer simulations of spectra of the triplet spectra with parameters given in Table 3. Positive features are in enhanced absorption (*a*) and negative features are in emission (*e*).

fulfilled. However, the fact that CT emission from these molecules is observed at all indicates that V_{DA} between DMJ$^{+\bullet}$ and An$^{-\bullet}$ is large, and since $2J \propto V_{DA}^2$, $2J$ is most likely much too large for the RP-ISC mechanism to occur.[49] Our TREPR results confirm this conclusion because RP-ISC followed by charge recombination to produce D−^{3*}A is selective with respect to the high-field eigenfunctions and not the molecular zero-field eigenfunctions as is the case for SO−ISC. Specifically, if the high-field T_0 triplet sublevel was overpopulated at all canonical orientations within DMJ−^{3*}An and DMJ−^{3*}An−tol, their triplet EPR spectra should exhibit an (*a*, *e*, *e*, *a*, *a*, *e*) polarization pattern, which is not the case, Figures 3B and 5.[93,95,96]

We similarly conclude that any contribution from direct SO−ISC operative in ^{1*}An → ^{3*}An is also negligible, because the ESP phase patterns observed for ^{3*}An are not observed for DMJ−^{3*}An and DMJ−^{3*}An−tol. However, an alternative spin−orbit mechanism that couples ^{1}(D$^{+\bullet}$−A$^{-\bullet}$) and D−^{3*}A has been suggested by several groups studying molecular CT complexes.[23,97−101] Iwata et al.[97] analyzed complexes between a 1,2,4,5-tetracyanobenzene acceptor and mesitylene, durene, and hexamethylbenzene donors at 77 K and found that the CT lifetime decreases as the donor ability increases. They concluded that CT complex formation created additional singlet−triplet mixing processes which resulted in faster decay of the CT complex. Similarly, Gould et al.[35] determined that rapid SO−ISC from the singlet exciplex results in direct population of the excited cyanoanthracene triplet in a series of exciplexes between cyanoanthracene acceptors and alkylbenzene donors. In these intermolecular CT complexes, the orientation and distances between D and A are not well defined, so that a detailed mechanistic understanding is difficult to determine.

TABLE 3: Zero-Field Splitting Parameters (*D* and *E*) and Relative Population Rates $a_{X,Y,Z}$ of the Zero-Field Spin States Obtained from Simulations of the Triplet-State TREPR Spectra of the Indicated Molecules in a Toluene Matrix at 85 K

molecule	*D* (mT)	*E* (mT)	A_X	A_Y	A_Z
An	77.81	−8.81	0.78	1.00	0.07
DMJ−An	74.96	−8.01	0.26	1.00	0.21
DMJ−An−tol	73.00	−7.56	0.45	1.00	0.32

In comparison, intramolecular D−A molecules provide relatively well-defined conformations and fixed distances. In these systems, if the orientation between the relevant orbitals of D and A is such that charge transfer between them is accompanied by a significant change in orbital angular momentum, recombination of ^{1}(D$^{+\bullet}$−A$^{-\bullet}$) may be accompanied by a spin flip to directly yield D−^{3*}A.[35,54,56] Okada et al.[54] discovered that the ISC rate in a covalently linked pyrene-*N*-methylaniline derivative was strongly dependent upon the relative orientation of the donor and acceptor groups. RP-ISC, which usually occurs on a time scale of a few nanoseconds, could not explain formation of a pyrene triplet state within 30 ps following photoexcitation of pyrene to its lowest excited singlet state. They concluded that when the electron donating and accepting molecular orbitals are approximately perpendicular to each other, the rate of ^{1}(D$^{+\bullet}$−A$^{-\bullet}$) → D−^{3*}A is increased. In this case the spin−orbit interaction does not result in ^{1}(D$^{+\bullet}$−A$^{-\bullet}$) →^{3}(D$^{+\bullet}$−A$^{-\bullet}$) because $\langle ^1(D^{+\bullet}-A^{-\bullet})|\mathscr{H}_{SO}|^3(D^{+\bullet}-A^{-\bullet})\rangle = 0$, due to the fact that there is no change in the spatial orbital for this process.[102] This mechanism is formally similar to rapid SO−ISC that occurs in an $n-\pi^*$ electronic transition within a single chromophore. However, because it requires a ^{1}(D$^{+\bullet}$−A$^{-\bullet}$) precursor, we will refer to it as spin−orbit, charge-transfer intersystem crossing (SOCT−ISC) for the remainder of this paper, so that the matrix element which describes this interaction is $\langle ^1(D^{+\bullet}-A^{-\bullet})|\mathscr{H}_{SOCT}|D-^{3*}A\rangle$.

Using TREPR, van Willigen et al.[56] studied 10-methylacridinium systems having arene electron donors attached to their 9-position. Although the ZFS parameters remained essentially constant, the relative population rates, A_X, A_Y, and A_Z, and thus the ESP phase pattern, were found to be a sensitive function of the orientation of the donor and acceptor π systems. They found that the SOCT−ISC rate was enhanced with an approximately perpendicular orientation between the donor and acceptor, $\theta_1 \approx 90°$. In another example, Wasielewski et al.[55] compared triplet formation between zinc porphyrins both isolated and serving as electron donors to which tetracyano-naphthoquinodimethane

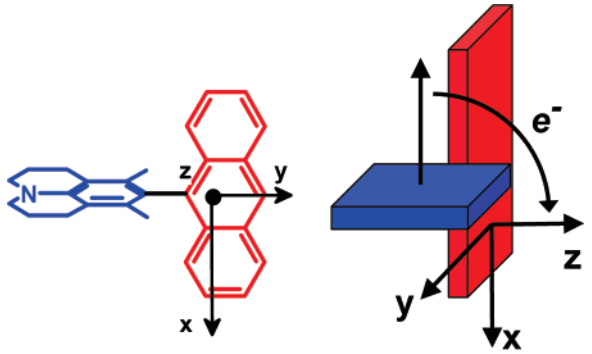

Figure 6. Charge transfer from DMJ to An in DMJ-An between orbitals oriented in the $x-z$ plane results in an angular momentum component along y. This angular momentum component coincides with SO−ISC to the corresponding spin sublevels of ^{3*}An.

acceptors were rigidly attached, so that the π systems of the donor and acceptor were oriented approximately 60° relative to one another. Following photoexcitation at 10 K, TREPR of the isolated zinc porphyrin revealed a porphyrin triplet state where SO−ISC exclusively populates the out-of-plane sublevel, T_Z, whereas in the D−A system, the porphyrin triplet state displayed an ESP pattern indicative of SOCT−ISC to the in-plane sublevels, T_X and T_Y. More recently, Dance et al.[44] showed that in addition to the dependence on orientation between the orbitals relevant to charge transfer, the magnitude of the electronic coupling between D and A strongly influences the contribution from the SOCT−ISC process. While studying a series of donor-bridge-acceptor (D−B-A) molecules where *D* = phenothiazine, *B* = a series of *p*-phenylene (Ph_n) oligomers, with $n = 1-5$, and *A* = perylene-3,4:9,10-bis(dicarboximide),[103] they found that with shorter bridge lengths the increased electronic coupling leads to a larger SOCT−ISC contribution producing D−B−^{3*}A.

In anthracene, the triplet axis system coincides with the lowest electronic transitions and is clearly dictated by the molecular structure, Figure 6.[104−106] Computer simulations of the triplet spectra for DMJ−^{3*}An and DMJ−^{3*}An−tol indicate that the (*e*, *a*, *e*, *a*, *e*, *a*) ESP phase pattern is the result of preferential population of the T_Y sublevel, Figure 3A, for $D > 0$, $E < 0$.[93,94] Charge transfer from DMJ to An involves moving an electron between two orbitals having a geometry change in the $x-z$ plane as defined in Figure 6. Using the right-hand rule, this implies that the angular momentum change is along the *y* direction, so that the SOCT interaction which couples ^{1}(D$^{+\bullet}$−A$^{-\bullet}$) and D−^{3*}A preferentially populates T_Y (i.e., $A_Y > A_{X,Z}$) of D−^{3*}A, as is observed in the TREPR spectra of the triplet states of DMJ−^{3*}An and DMJ−^{3*}An−tol, Table 3.[107,108] Although T_Y is preferentially populated in both cases, there is an increase of the A_X and A_Z population rates in DMJ−^{3*}An−tol relative to DMJ−^{3*}An. This suggests that conjugation between the anthracene and the phenyl group relaxes the symmetry restrictions in a way that alters the sublevel population rates.

Absence of a Triplet State TREPR Spectrum in J−An. It is particularly interesting that J−An has a very low triplet yield and consequently its triplet EPR spectrum is not observed following photoexcitation despite its obvious similarity to DMJ−An. As discussed above, SOCT−ISC requires a ^{1}(D$^{+\bullet}$−A$^{-\bullet}$) precursor and depends strongly on the orientation of the molecular orbitals involved in the charge transfer as well as the magnitude of V_{DA}.[35,55,57,106,109,110] The solvatochromism data for J−An, DMJ−An, and DMJ−An−tol show that the formation of ^{1}(D$^{+\bullet}$−A$^{-\bullet}$) is essentially quantitative for all three molecules. Thus, the differences in triplet intersystem crossing

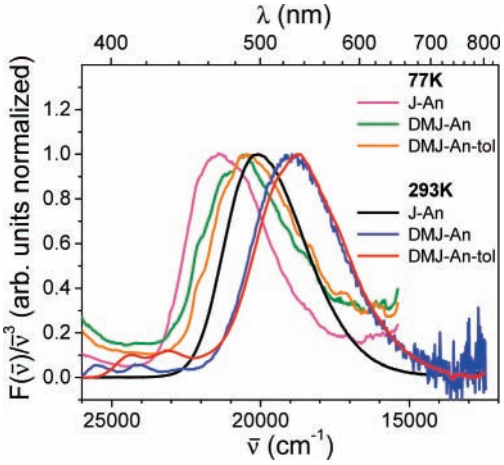

Figure 7. Fluorescence spectra of the indicated molecules in toluene at 293 and 77 K. The spectra are normalized at their maxima.

rates most likely depend on differences in V_{DA} and donor−acceptor orbital orientation. Our results show that even when $\theta_1 \approx 90°$, as is the case for DMJ−An and DMJ−An−tol, V_{DA} is large enough to enable SOCT−ISC to occur at a rate sufficient to produce a high yield of DMJ−^{3*}An and DMJ−^{3*}An−tol. Thus it is likely that the negligible yield of J−^{3*}An results from the diminished change in orbital angular momentum that occurs between the π systems of J and An, when θ_1 deviates from 90°.

Participation of the Anthracene Triplet LE states in ISC. To account for the solvent and temperature dependence of the CT emission of ADMA and its derivatives, it has been shown that it is necessary to include mixing with an energetically proximate, symmetry-allowed ^{1}LE state of An.[1,3,10,18,37,38,111] In considering the mechanism of ISC within the analogous systems discussed here, we must also consider contributions from energetically relevant triplet ^{3}LE states of An. The smaller value of k_{ISC} for DMJ−An−tol relative to that of DMJ−An is consistent with similar observations on the effects of conjugated substituents at the 9,10-positions of An on these rate constants.[24−33] Anthracene itself undergoes efficient SO−ISC because the energy of its T_2 state at 3.22 eV is about 0.06 eV below that of S_1.[24,27,32,33] This SO−ISC process ($S_1 \rightarrow T_2 \rightarrow T_1$) occurs in fluid solution at 295 K as well as in a frozen solvent matrix at 77 K. Placing conjugated substituents at the 9- and/or 10-positions may reverse this energy ordering, so that S_1 is below T_2.[24,27,32,33] For example, this reversal is responsible for the dramatic decrease in the ISC rate of 9,10-diphenylanthracene relative to that of anthracene.[24,28]

Our results show that the energies of ^{1}(DMJ$^{+\bullet}$−An$^{-\bullet}$) and ^{1}(DMJ$^{+\bullet}$−An$^{-\bullet}$−tol) are 2.83 and 2.75 eV at 293 K, well below that of the pure LE T_2 (3.22 eV) state of anthracene and significantly above its T_1 state (1.83 eV).[33,86,112] Under these conditions, SOCT−ISC via T_2 (similar to anthracene) becomes a strongly activated process, so that significant population of T_2 is unlikely. However, our TREPR results were obtained at 85 K in a frozen toluene matrix, where solvent reorganization is inhibited, so that the energies of ^{1}(DMJ$^{+\bullet}$−An$^{-\bullet}$) and ^{1}(DMJ$^{+\bullet}$−An$^{-\bullet}$−tol) are higher because they are no longer stabilized by solvent dipole reorientation.[113,114] The fluorescence spectra of J−An, DMJ−An, and DMJ−An−tol indicate that their CT state energy levels all increase by ~0.2 eV upon cooling from 293 to 77 K in toluene, Figure 7. This change places the energies of ^{1}(DMJ$^{+\bullet}$−An$^{-\bullet}$) and ^{1}(DMJ$^{+\bullet}$−An$^{-\bullet}$−tol) much closer to that of the T_2 LE state of An. Thus, the SOCT−ISC process at 85K most likely has a contribution from the

matrix element involving the T_2 state of An, $\langle {}^1(D^{+\bullet}-A^{-\bullet}) |\mathscr{H}_{SOCT}| D-{}^{3*}A(T_2)\rangle$, in addition to a contribution from the corresponding matrix element involving T_1, $\langle {}^1(D^{+\bullet}-A^{-\bullet}) |\mathscr{H}_{SOCT}| D-{}^{3*}A(T_1)\rangle$.

Conclusions

TREPR studies show that the primary mechanism of triplet formation in DMJ−An and DMJ−An−tol following photoexcitation is the SOCT−ISC mechanism, which is similar to that which occurs in an $n-\pi^*$ electronic transition within a single chromophore. The SOCT−ISC mechanism is characterized by the (*e*, *a*, *e*, *a*, *e*, *a*) ESP phase pattern in the DMJ−^{3*}An and DMJ−^{3*}An−tol TREPR spectra and depends on the degree of charge separation, the relative orientation of the orbitals involved in the charge transfer, and the magnitude of the electronic coupling between the donor and acceptor. In J−An, DMJ−An, and DMJ−An−tol, where the donor and acceptor are formally linked by a single bond, all of these parameters depend on the torsional angle (θ_1) between the π system of the anthracene and the phenyl of the julolidine. Despite its similar structure, photoexcitation of J−An produces a very low triplet yield. This results from the decrease in θ_1 in the $^1(J^{+\bullet}-An^{-\bullet})$ state due to the absence of the 3,5-dimethyl substituents on julolidine. Although this decrease is most likely only about 15−30° relative to that of $^1(DMJ^{+\bullet}-An^{-\bullet})$ and $^1(DMJ^{+\bullet}-An^{-\bullet}-tol)$, it is sufficient to significantly decrease SOCT−ISC for J−An by decreasing the change in orbital angular momentum accompanying charge transfer. Given that the requirements for the SOCT−ISC mechanism are quite general, we expect it to occur in a variety of electron donor−acceptor systems in which the donor π system is structurally restricted to a nearly perpendicular orientation relative to that of the acceptor.

Acknowledgment. This work was supported by the Chemical Sciences, Geosciences, and Biosciences Division, Office of Basic Energy Sciences, U.S. Department of Energy under Grant DE-FG02-99ER14999 (MRW) and the NSF and ONR Chemistry Divisions (MAR).

Supporting Information Available: Synthesis of compounds; Figures S1 and S2 (PDF). This material is available free of charge via the Internet at http://pubs.acs.org.

References and Notes

(1) Grabowski, Z. R.; Rotkiewicz, K.; Rettig, W. *Chem. Rev.* **2003**, *103*, 3899−4031.
(2) Herbich, J.; Kapturkiewicz, A. *Chem. Phys.* **1991**, *158*, 143−153.
(3) Herbich, J.; Kapturkiewicz, A. *Chem. Phys. Lett.* **1997**, *273*, 9−17.
(4) Kapturkiewicz, A. *Chem. Phys.* **1992**, *166*, 259−273.
(5) Mataga, N.; Nishikawa, S.; Asahi, T.; Okada, T. *J. Phys. Chem.* **1990**, *94*, 1443−1447.
(6) Nagarajan, V.; Brearley, A. M.; Kang, T. J.; Barbara, P. F. *J. Chem. Phys.* **1987**, *86*, 3183−3196.
(7) Okada, T.; Fujita, T.; Kubota, M.; Masaki, S.; Mataga, N.; Ide, R.; Sakata, Y.; Misumi, S. *Chem. Phys. Lett.* **1972**, *14*, 563−568.
(8) Okada, T.; Fujita, T.; Mataga, N. *Z. Phys. Chem. N. F.* **1976**, *101*, 57−66.
(9) Siemiarczuk, A. *Chem. Phys. Lett.* **1984**, *110*, 437.
(10) Siemiarczuk, A.; Ware, W. R. *J. Phys. Chem.* **1987**, *91*, 3677−3682.
(11) Siemiarczuk, A.; Grabowski, Z. R.; Krowczynski, A.; Asher, M.; Ottolenghi, M. *Chem. Phys. Lett.* **1977**, *51*, 315−320.
(12) Siemiarczuk, A.; Koput, J.; Pohorille, A. *Z. Naturforsch* **1982**, *A37*, 598.
(13) Tominaga, K.; Walker, G. C.; Jarzeba, W.; Barbara, P. F. *J. Phys. Chem.* **1991**, *95*, 10475−10485.
(14) Tominaga, K.; Walker, G. C.; Kang, T. J.; Barbara, P. F.; Fonseca, T. *J. Phys. Chem.* **1991**, *95*, 10485−10492.
(15) Menzel, R.; Windsor, M. W. *Chem. Phys. Lett.* **1991**, *184*, 6−10.
(16) Okada, T.; Nakatani, K.; Hagihara, M.; Mataga, N. In *Ultrafast Phenomena VI*; Springer Series in Chemical Physics; Springer Verlag: Berlin, 1988; Vol. 48, pp 555−558.
(17) Okada, T.; Mataga, N.; Baumann, W.; Siemiarczuk, A. *J. Phys. Chem.* **1987**, *91*, 4490−4495.
(18) Herbich, J.; Kapturkiewicz, A. *J. Am. Chem. Soc.* **1998**, *120*, 1014−1029.
(19) Grabowski, Z. R.; Rotkiewicz, K.; Siemiarczuk, A.; Cowley, D. J.; Baumann, W. *Nouv. J. Chim.* **1979**, *3*, 443−454.
(20) Lee, S.; Arita, K.; Kajimoto, O.; Tamao, K. *J. Phys. Chem. A* **1997**, *101*, 5228−5231.
(21) Lee, S.; Kajimoto, O. *J. Phys. Chem. A* **1997**, *101*, 5232−5240.
(22) Martin, M. M.; Plaza, P.; Changenet-Barret, P.; Siemiarczuk, A. *J. Phys. Chem. A* **2002**, *106*, 2351−2358.
(23) Ottolenghi, M.; Goldschmidt, C. R.; Potashnik, R. *J. Phys. Chem.* **1971**, *75*, 1025−1031.
(24) Hirayama, S.; Lampert, R. A.; Phillips, D. *J. Chem. Soc., Faraday Trans. I* **1985**, *81*, 371−382.
(25) Lampert, R. A.; Phillips, D. *J. Chem. Soc., Faraday Trans. I* **1985**, *81*, 383−393.
(26) Tanaka, M.; Tanaka, I.; Tai, S.; Hamanoue, K.; Sumitani, M.; Yoshihara, K. *J. Phys. Chem.* **1983**, *87*, 813−816.
(27) Nijegorodov, N. I.; Downey, W. S. *Spectrochim. Acta, Part A* **1995**, *51*, 2335−2346.
(28) Nijegorodov, N. I.; Downey, W. S. *J. Phys. Chem.* **1994**, *98*, 5639−5643.
(29) Hamanoue, K.; Hirayama, S.; Nakayama, T.; Teranishi, H. *Chem. Lett.* **1980**, 407−410.
(30) Wu, K. C.; Ware, W. R. *J. Am. Chem. Soc.* **1979**, *101*, 5906−5909.
(31) Lim, E. C.; Laposa, J. D.; Yu, J. M. H. *J. Mol. Spectrosc.* **1966**, *19*, 412-&.
(32) Tanaka, F.; Okamoto, M.; Hirayama, S. *J. Phys. Chem.* **1995**, *99*, 525−530.
(33) Fukumura, H.; Kikuchi, K.; Koike, K.; Kokubun, H. *J. Photochem. Photobiol., A* **1988**, *42*, 283−291.
(34) Hirayama, S. *J. Chem. Soc., Faraday Trans. I* **1982**, *78*, 2411−2421.
(35) Gould, I. R.; Boiani, J. A.; Gaillard, E. B.; Goodman, J. L.; Farid, S. *J. Phys. Chem. A* **2003**, *107*, 3515−3524.
(36) Tsubomura, H.; Mulliken, R. S. *J. Am. Chem. Soc.* **1960**, *82*, 5966−5974.
(37) Murrell, J. N. *J. Am. Chem. Soc.* **1959**, *81*, 5037−5043.
(38) Mulliken, R. S. *J. Am. Chem. Soc.* **1950**, *72*, 600−608.
(39) Bixon, M.; Jortner, J.; Verhoeven, J. W. *J. Am. Chem. Soc.* **1994**, *116*, 7349−7355.
(40) Weller, A.; Staerk, H.; Treichel, R. *Faraday Discuss. Chem. Soc.* **1984**, *78*, 271−278.
(41) Hoff, A. J.; Gast, P.; van der Vos, R.; Franken, E. M.; Lous, E. J. *Z. Phys. Chem.* **1993**, *180*, 175−192.
(42) Till, U.; Hore, P. J. *Mol. Phys.* **1997**, *90*, 289−296.
(43) Steiner, U. E.; Ulrich, T. *Chem. Rev.* **1989**, *89*, 51−147.
(44) Dance, Z. E. X.; Mi, Q. X.; McCamant, D. W.; Ahrens, M. J.; Ratner, M. A.; Wasielewski, M. R. *J. Phys. Chem. B* **2006**, *110*, 25163−25173.
(45) Schulten, K.; Staerk, H.; Weller, A.; Werner, H.-J.; Nickel, B. *Z. Phys. Chem.* **1976**, *101*, 371−390.
(46) Tanimoto, Y.; Okada, N.; Itoh, M.; Iwai, K.; Sugioka, K.; Takemura, F.; Nakagaki, R.; Nagakura, S. *Chem. Phys. Lett.* **1987**, *136*, 42−46.
(47) Sakaguchi, Y.; Hayashi, H. *J. Phys. Chem. A* **1997**, *101*, 549−555.
(48) Werner, U.; Kuhnle, W.; Staerk, H. *J. Phys. Chem.* **1993**, *97*, 9280−9287.
(49) Weiss, E. A.; Ratner, M. A.; Wasielewski, M. R. *J. Phys. Chem. A* **2003**, *107*, 3639−3647.
(50) Weiss, E. A.; Ahrens, M. J.; Sinks, L. E.; Gusev, A. V.; Ratner, M. A.; Wasielewski, M. R. *J. Am. Chem. Soc.* **2004**, *126*, 5577−5584.
(51) Lukas, A. S.; Bushard, P. J.; Weiss, E. A.; Wasielewski, M. R. *J. Am. Chem. Soc.* **2003**, *125*, 3921−3930.
(52) Tadjikov, B.; Smirnov, S. *Phys. Chem. Chem. Phys.* **2001**, *3*, 204−212.
(53) Tsentalovich, Y. P.; Morozova, O., B.; Avdievich, N. I.; Ananchenko, G. S.; Yurkovskaya, A. V.; Ball, J. D.; Forbes, M. D. E. *J. Phys. Chem. A* **1997**, *101*, 8809−8816.
(54) Okada, T.; Karaki, I.; Matsuzawa, E.; Mataga, N.; Sakata, Y.; Misumi, S. *J. Phys. Chem.* **1981**, *85*, 3957−3960.
(55) Wasielewski, M. R.; Johnson, D. G.; Svec, W. A.; Kersey, K. M.; Minsek, D. W. *J. Am. Chem. Soc.* **1988**, *110*, 7219−7221.
(56) van Willigen, H.; Jones, G., II; Farahat, M. S. *J. Phys. Chem.* **1996**, *100*, 3312−3316.
(57) Khudyakov, I. V.; Serebrennikov, Y. A.; Turro, N. J. *Chem. Rev.* **1993**, *93*, 537−570.
(58) Lin, T. S. *Chem. Rev.* **1984**, *84*, 1−15.

(59) Yagi, M.; Shirai, H.; Ohta, J.; Higuchi, J. *Chem. Phys. Lett.* **1989**, *160*, 13−16.
(60) Krzystek, J. *Org. Magn. Reson.* **1980**, *13*, 151−152.
(61) Hayashi, H.; Iwata, S.; Nagakura, S. *J. Chem. Phys.* **1969**, *50*, 993−1000.
(62) Hayashi, H.; Nagakura, S.; Iwata, S. *Mol. Phys.* **1967**, *13*, 489−490.
(63) Kamata, Y.; Akiyama, K.; Tero-Kubota, S. *J. Phys. Chem. A* **1999**, *103*, 1714−1718.
(64) Mclauchlan, K. A.; Shkrob, I. A.; Yeung, M. T. *Chem. Phys. Lett.* **1994**, *217*, 157−162.
(65) Hasharoni, K.; Levanon, H.; Greenfield, S. R.; Gosztola, D. J.; Svec, W. A.; Wasielewski, M. R. *J. Am. Chem. Soc.* **1995**, *117*, 8055−8056.
(66) Levanon, H.; Galili, T.; Regev, A.; Wiederrecht, G. P.; Svec, W.; Wasielewski, M. R. *J. Am. Chem. Soc.* **1998**, *120*, 6366−6373.
(67) Shaakov, S.; Galili, T.; Stavitski, E.; Levanon, H.; Lukas, A. S.; Wasielewski, M. R. *J. Am. Chem. Soc.* **2003**, *125*, 6563−6572.
(68) Wiederrecht, G. P.; Svec, W. A.; Wasielewski, M. R. *J. Am. Chem. Soc.* **1999**, *121*, 7726−7727.
(69) Kawai, A.; Okutsu, T.; Obi, K. *Chem. Phys. Lett.* **1995**, *235*, 450−455.
(70) Hutchinson, C. A.; Mangum, B. W. *J. Chem. Phys.* **1958**, *29*, 952−953.
(71) Hutchinson, C. A.; Mangum, B. W. *J. Chem. Phys.* **1961**, *34*, 908−922.
(72) Wasserman, E.; Snyder, L. C.; Yager, W. A. *J. Chem. Phys.* **1964**, *41*, 1763−1772.
(73) Blank, A.; Levanon, H. *Concepts Magn. Reson., Part A* **2005**, *25*, 18−39.
(74) Levanon, H.; Norris, J. R. *Chem. Rev.* **1978**, *78*, 185−198.
(75) Crosby, G. A.; Demas, J. N. *J. Phys. Chem.* **1971**, *75*, 991−1024.
(76) Pshenichnikov, M. S.; de Boerij, W. P.; Wiersma, D. A. *Opt. Lett.* **1994**, *19*, 572−575.
(77) Pavlopoulos, T. G. *J. Appl. Phys.* **1992**, *72*, 845−848.
(78) *MATLAB*; The MathWorks, Inc.: Natick, MA, 2006.
(79) Angulo, G.; Grampp, G.; Rosspeintner, A. *Spectrochim. Acta, Part A* **2006**, *65A*, 727−731.
(80) Lippert, E. Z. *Naturforsch.* **1955**, *10a*, 541−546.
(81) Mataga, N.; Kaifu, Y.; Koizumi, M. *Bull. Chem. Soc. Jpn.* **1956**, *29*, 465−470.
(82) *Hyperchem*; Hypercube Inc.: Gainesville, FL.
(83) Frisch, M. J.; Trucks, G. W.; Schlegel, H. B.; Scuseria, G. E.; Robb, M. A.; Cheeseman, J. R.; Zakrzewski, V. G.; Montgomery, J. A.; Stratmann, R. E.; Burant, J. C.; Dapprich, S.; Millam, J. M.; Daniels, A. D.; Kudin, K. N.; Strain, M. C.; Farkas, O.; Tomasi, J.; Barone, V.; Cossi, M.; Cammi, R.; Mennucci, B.; Pomelli, C.; Adamo, C.; Clifford, S.; Ochterski, J.; Petersson, G. A.; Ayala, P. Y.; Cui, Q.; Morokuma, K.; Malick, D. K.; Rabuck, A. D.; Raghavachari, K.; Foresman, J. B.; Cioslowski, J.; Ortiz, J. V.; Stefanov, B. B.; Liu, G.; Liashenko, A.; Piskorz, P.; Komaromi, I.; Gomperts, R.; Martin, R. L.; Fox, D. J.; Keith, T.; Al-Laham, M. A.; Peng, C. Y.; Nanayakkara, A.; Gonzalez, C.; Challacombe, M.; Gill, P. M. W.; Johnson, B. G.; Chen, W.; Wong, M. W.; Andres, J. L.; Head-Gordon, M.; Replogle, E. S.; Pople, J. A. *Gaussian*, version 5.2; Gaussian, Inc.: Pittsburgh, PA, 1998.
(84) Becke, A. D. *J. Chem. Phys.* **1993**, *98*, 1372−1377.
(85) Lee, C.; Yang, W.; Parr, R. G. *Phys. Rev. B* **1988**, *37*, 785−789.
(86) Tanaka, F.; Osugi, J. *Chem. Phys. Lett.* **1974**, *27*, 133−137.
(87) Hunter, T. F.; Wyatt, R. F. *Chem. Phys. Lett.* **1970**, *6*, 221−224.
(88) Kellogg, R. E. *J. Chem. Phys.* **1966**, *44*, 411−412.
(89) Bohne, C.; Kennedy, S. R.; Boch, R.; Negri, F.; Orlandi, G.; Siebrand, W.; Scaiano, J. C. *J. Phys. Chem.* **1991**, *95*, 10300−10306.
(90) Hamanoue, K.; Hirayama, S.; Nakayama, T.; Teranishi, H. *J. Phys. Chem.* **1980**, *84*, 2074−2078.
(91) Antheunis, D. A.; Schmidt, J.; van der Waals, J. H. *Mol. Phys.* **1974**, *27*, 1521−1541.
(92) van der Waals, J. H.; ter Maten, G. *Mol. Phys.* **1964**, *8*, 301.
(93) Thurnauer, M. C. *Rev. Chem. Interm.* **1979**, *3*, 197−230.
(94) Thurnauer, M. C.; Katz, J. J.; Norris, J. R. *Proc. Natl. Acad. Sci. U.S.A.* **1975**, *72*, 3270−3274.
(95) Dutton, P. L.; Leigh, J. S.; Reed, D. W. *Biochim. Biophys. Acta* **1973**, *292*, 654−664.
(96) Dutton, P. L.; Leigh, J. S.; Seibert, M. *Biochem. Biophys. Res. Commun.* **1972**, *46*, 406−413.
(97) Iwata, S.; Tanaka, J.; Nagakura, S. *J. Chem. Phys.* **1967**, *47*, 2203−2209.
(98) Christodouleas, N. D.; McGlynn, S. P. *J. Chem. Phys.* **1964**, *40*, 166−174.
(99) Webster, D.; Baugher, J. F.; Lim, B. T.; Lim, E. C. *Chem. Phys. Lett.* **1981**, *77*, 294−298.
(100) Chandra, A. K.; Lim, E. C. *Chem. Phys. Lett.* **1977**, *45*, 79−83.
(101) van der Auweraer, M.; Grabowski, Z. R.; Rettig, W. *J. Phys. Chem.* **1991**, *95*, 2083−2092.
(102) Lim, B. T.; Okajima, S.; Chandra, A. K.; Lim, E. C. *Chem. Phys. Lett.* **1981**, *79*, 22−27.
(103) van der Boom, T.; Hayes, R. T.; Zhao, Y.; Bushard, P. J.; Weiss, E. A.; Wasielewski, M. R. *J. Am. Chem. Soc.* **2002**, *124*, 9582−9590.
(104) Siegel, S.; Goldstein, L. *J. Chem. Phys.* **1965**, *43*, 4185−4187.
(105) Siegel, S.; Judeikis, H. S. *J. Phys. Chem.* **1965**, *70*, 2205−2211.
(106) El-Sayed, M. A. *J. Chem. Phys.* **1974**, *60*, 4502−4507.
(107) van der Waals, J. H.; de Groot, M. S. In *The Triplet State*; Zahlan, A. B., Ed.; University Press: Cambridge, U.K., 1967; pp 101−132.
(108) El-Sayed, M. A., Lim, E. C., Ed.; Academic Press: New York, 1974; Vol. 1, pp 35−77.
(109) Salem, L.; Rowland, C. *Angew. Chem., Int. Ed.* **1972**, *11*, 92−111.
(110) Morais, J.; Hung, R. R.; Grabowski, J. J.; Zimmt, M. B. *J. Phys. Chem.* **1993**, *97*, 13138−13144.
(111) Bixon, M.; Jortner, J.; Cortes, J.; Heitele, H.; Michel-Beyerle, M. E. *J. Phys. Chem.* **1994**, *98*, 7289−7299.
(112) Langelaar, J.; Rettschnick, R. P. H.; Hoijtink, G. J. *J. Chem. Phys.* **1971**, *54*, 1−7.
(113) Gaines, G. L., III; O'Neil, M. P.; Svec, W. A.; Niemczyk, M. P.; Wasielewski, M. R. *J. Am. Chem. Soc.* **1991**, *113*, 719−721.
(114) Marcus, R. A. *J. Phys. Chem.* **1990**, *94*, 4963−4966.